Evidence for Dyakonov-Perel-like Spin Relaxation in Pt

Ryan Freeman,[1] Andrei Zholud,[1] Zhiling Dun,[2] Haidong Zhou,[2] and Sergei Urazhdin[1]
[1]Department of Physics, Emory University, Atlanta, Georgia 30322, USA
[2]Department of Physics and Astronomy, University of Tennessee, Knoxville, Tennessee 37996, USA

(Received 17 July 2017; revised manuscript received 30 October 2017; published 9 February 2018)

We utilize nanoscale spin valves with Pt spacer layers to characterize spin relaxation in Pt. Analysis of the spin lifetime indicates that Elliott-Yafet spin scattering is dominant at room temperature, but an unexpected intrinsic Dyakonov-Perel-like spin relaxation becomes dominant at cryogenic temperatures. We also observe suppression of spin relaxation in a Pt layer interfaced with a ferromagnet, likely caused by the competition between the effective exchange and spin-orbit fields.

DOI: 10.1103/PhysRevLett.120.067204

The interplay between the electron's motion and its spin, due to the spin-orbit interaction (SOI), opens unprecedented opportunities for the control of both spin and orbital degrees of freedom [1–5]. For instance, the spin Hall effect (SHE) results in generation of pure spin current [6], enabling electronic control of magnetization in metallic and insulating nanomagnets [7–9]. Recent studies of materials that exhibit large SOI, including Pt, Ta, W, topological insulators, and alloys such as CuBi, have focused on identifying the SOI mechanisms, and characterizing the relevant parameters, including the spin-orbit scattering rates, the spin Hall angle, and the effective spin-orbit field [10–17]. Another relevant parameter is the spin diffusion length λ, defined as the length scale for the relaxation of spin polarization away from its source. It is also the length scale for spin current generation via the SHE, and is thus directly related to SHE efficiency.

Pt is one of the most extensively studied spin-orbit materials, thanks to the large SOI effects [10,18,19], and relatively low resistivity minimizing Joule heating and current shunting in heterostructures. Parameters relevant to SOI in Pt such as the spin Hall angle and λ have been studied by a variety of techniques [10,14,18,20–22]. Nevertheless, the values and the mechanisms controlling them are still debated. In particular, the reported values of the spin Hall angle in Pt range from 0.004 to over 0.1 [10,14,23], and those of λ range from less than 1 nm to over 10 nm [10,14,18,20–22,24–26]. Such a large spread of the reported characteristics makes it challenging to establish the mechanisms controlling the spin-orbit effects.

One of the main difficulties in analyzing SOI is posed by the interplay between interfacial and bulk effects. For instance, the apparent spin Hall angle in a SHE-ferromagnet bilayer depends on the transparency of their interface [23,27,28]. Measurements of λ based on the spin absorption efficiency are similarly affected by the spin relaxation at the interfaces [21]. Furthermore, the spin-orbit effects at interfaces with ferromagnets may be affected by the temperature-dependent contribution from the proximity-induced magnetism [29].

One approach that can unambiguously separate the interfacial from the bulk contributions to spin relaxation is based on the current-perpendicular-to-plane giant magnetoresistance (CPP-GMR) in ferromagnet–normal-metal–ferromagnet (F-N-F) spin valves, with the studied material inserted in the spacer N [30]. The value of λ is directly determined from the dependence of GMR on the material thickness, while the contribution of the interfaces is determined from the dependence on the number of inserted spacers. In CPP-GMR, electrical current flows normal to the studied layer, and therefore electron transport is described by the bulk material parameters even for ultrathin films. In contrast, techniques based on the in-plane current flow require an elaborate analysis of thickness-dependent resistivities and current shunting [25,26]. Although the GMR-based approach to the quantitative characterization of spin scattering in materials is well established, only one such measurement has been reported for Pt at temperature $T = 4.2$ K [25], yielding the value of λ significantly larger than those obtained with other approaches [18].

Here, we report a study of the temperature-dependent GMR in nanopillar spin valves with Pt spacers, and demonstrate that this approach can be utilized to elucidate the mechanisms of spin scattering in Pt and at its interfaces, and to characterize the relevant spin-orbit parameters. The dependence of GMR on the Pt spacer thickness allowed us to determine the value of λ and extract the spin lifetime. The observed temperature dependence indicates that at room temperature, spin relaxation in the studied Pt films is dominated by the Elliott-Yafet (EY) scattering, while at cryogenic temperatures it is dominated by intrinsic spin dephasing that can be attributed to the presence of an effective spin-orbit field. We also demonstrate that spin relaxation is suppressed in a thin Pt layer interfaced with a ferromagnet, consistent with the competition between the

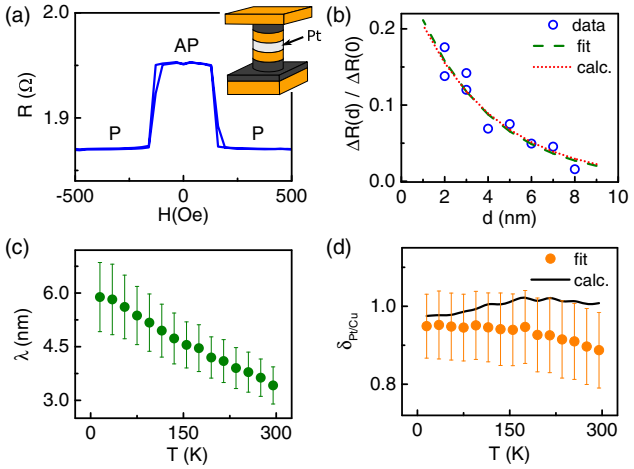

FIG. 1. (a) Resistance vs applied field for a sample without Pt spacer, at room temperature (RT), $T = 295$ K. Inset: schematic of the studied nanopillars, with Py layers shown in black, Cu in orange, and Pt in white. (b) Symbols: ΔR, scaled by the MR of the reference sample without Pt spacer, vs Pt thickness d, at RT. Dashed curve: exponential fit to the data. Dotted curve: calculation based on the Valet-Fert theory. (c) Spin diffusion length vs temperature, determined by fitting $\Delta R(d)$ with Eq. (1). (d) Interfacial spin-loss factor vs temperature, obtained by fitting $\Delta R(d)$ with Eq. (1) (symbols), and by minimizing the difference between the MR data and the Valet-Fert calculations (curve).

effective spin-orbit field and the proximity-induced exchange field in Pt.

The studied structures [inset in Fig. 1(a)] were based on multilayers Cu(40)Py(10)Cu(6-d/2)Pt(d)Cu(6-d/2)Py(5)Au(5), where Py = $Ni_{80}Fe_{20}$, and thicknesses are given in nanometers. The thickness d of the Pt insert was varied between 0 and 8 nm in 1 nm increments, with $d = 0$ representing the reference Py/Cu/Py nanopillar. The rms roughness of the multilayers was 0.3 nm. We excluded the sample with $d = 1$ nm from our analysis, because of the possible discontinuity of the 1 nm-thick Pt layer. The thickness of the Cu spacers separating Pt from the magnetic Py layers was at least 2 nm, to avoid proximity-induced magnetism in Pt [31,32]. A structure where Pt was directly interfaced with Py to analyze this effect is separately discussed below. The Py(5) layer, the nonmagnetic Cu/Pt/Cu spacer, and 5 nm of the bottom Py(10) were patterned into a circular 75 nm disk, while the rest of the structure was a micrometer-scale film.

The magnetizations of the Py layers formed antiparallel (AP) configuration with resistance R_{AP} at small field H, due to their antiferromagnetic dipolar coupling [33]. At large fields, both magnetizations became aligned into a parallel (P) configuration with resistance R_P, resulting in switching between P and AP states in field scans [Fig. 1(a)]. At a given temperature T the dependence of magnetoresistance (MR), $\Delta R = R_{AP} - R_P$, on d was well approximated by the exponential

$$\Delta R(d) = \Delta R(0) e^{-d/\lambda - 2\delta_{Pt/Cu}}, \quad (1)$$

as shown by the dashed curve in Fig. 1(b) for room temperature (RT), $T = 295$ K. Here, $\delta_{Pt/Cu}$ is the parameter describing spin loss at the Pt/Cu interface [15,23,34]. The temperature dependencies of λ and $\delta_{Pt/Cu}$, determined by fitting the dependence of MR on d with Eq. (1) at each T, are shown by symbols in Figs. 1(c) and 1(d), respectively. The value of λ increased from 3.5 nm at RT to 6.0 nm at 7 K [Fig. 1(c)]. The slight increase of $\delta_{Pt/Cu}$from 0.89 at RT to 0.95 at 7 K was within the fitting uncertainty.

Although the value of $\delta_{Pt/Cu}$ is not central to our study, we briefly discuss it here. This parameter is generally well defined only for diffuse interfaces, $\delta = w/\lambda_I$, where w is the width of the interfacial region, and λ_I is the effective spin diffusion length [15]. To establish whether this interpretation is consistent with the fitting using Eq. (1), we performed calculations based on the Valet-Fert (VF) theory of GMR [35–37], using the extracted λ and the known spin-dependent transport properties of Py, Cu and their interfaces [18,38]. We obtained $\delta_{Pt/Cu}$ by minimizing the difference between our data and the calculated MR [39]. The calculated dependence of MR on d reproduced the exponential form Eq. (1) [dotted curve in Fig. 1(b)], and the obtained $\delta_{Pt/Cu}$ [curve in Fig. 1(d)] is close to the result of simple exponential fitting, and to the value obtained for macroscopic spin valves at 4.2 K [47]. Based on these data, we conclude that the spin relaxation rate at the Cu/Pt interface is approximately temperature-independent. The overall agreement between the VF calculations and the fitting based on Eq. (1) validates our interpretation of λ and $\delta_{Pt/Cu}$ in terms of the bulk and interfacial contributions to spin diffusion across Pt layers. We emphasize that VF calculations are not needed to extract these parameters, reflecting the robust model-independent nature of the CPP-GMR technique.

Two distinct spin-orbit mechanisms can contribute to spin relaxation in materials and at their interfaces. EY relaxation is caused by scattering on phonons and impurities in the presence of spin-orbit band mixing, resulting in a linear relationship between the spin-flip time, τ_{sf}, and the momentum scattering time, τ_p [48]. Dyakonov-Perel (DP) relaxation is associated with spin precession around the effective spin-orbit field, $\vec{H}_{SO}$, at interfaces and in materials with broken inversion symmetry [27,28,48–51]. Spin dephasing caused by the dependence of $\vec{H}_{SO}$ on the electron's momentum results in the inverse relation between τ_{sf} and τ_p [49] for DP relaxation.

To analyze the spin relaxation in Pt, we determined the momentum scattering time, $\tau_p = m/\rho n e^2$, from the resistivity $\rho(T)$ [Fig. 2(a)] [39], which is typical for sputtered Pt films [10,18]. Here, m and e are the electron's mass and charge, and $n = 2.81 \times 10^{29}$ m^{-3} is the carrier concentration determined by the Hall measurement [39]. Figure 2(b)

shows the temperature dependence of the spin-flip time τ_{sf}, determined from λ [Fig. 1(c)] using $\lambda = \sqrt{v_F l \tau_{sf}/3}$ [18], where $v_F = \sqrt[3]{3\pi^2 n\hbar/m}$ is the Fermi velocity, and $l = v_F \tau_p$ is the mean free path. Significantly larger values of τ_{sf} were obtained for Pt from the Hanle-type measurements [52], likely because such measurements are dominated by the low-mobility carriers whose spin relaxation can be significantly slower than that of high-mobility carriers in transport phenomena [53].

At high temperatures, both τ_p and τ_{sf} in Figs. 2(a),2(b) linearly increase with decreasing T, consistent with the dominance of the EY mechanism. While the dependence $\tau_p(T)$ remains monotonic at low T, τ_{sf} starts to decrease. This decrease of τ_{sf} with increasing τ_p [Fig. 2(c)] is reminiscent of the DP mechanism, which is not allowed in Pt by symmetry. We emphasize that the CPP-GMR approach allows us to unambiguously attribute this to the bulk spin relaxation; if it were caused by the interfacial effects, this would have been captured by an increase of $\delta_{Pt/Cu}(T)$ [Fig. 1(d)].

The DP relaxation at Pt interfaces is allowed by symmetry [28]. However, the bulk DP mechanism is prohibited, so the spin relaxation in Pt has been attributed to the EY mechanism [10,21,26]. Increased spin relaxation observed at low temperatures in measurements of spin transport along Ag and Cu nanowires [54–56] has been explained by the increased contribution of surface scattering, when the mean free path becomes large. In CPP-GMR, current flows normal to the film, so this effect is not relevant. We can also eliminate the effects of magnetic fluctuations in Pt, which are too small to explain the observed enhancement of spin relaxation [39].

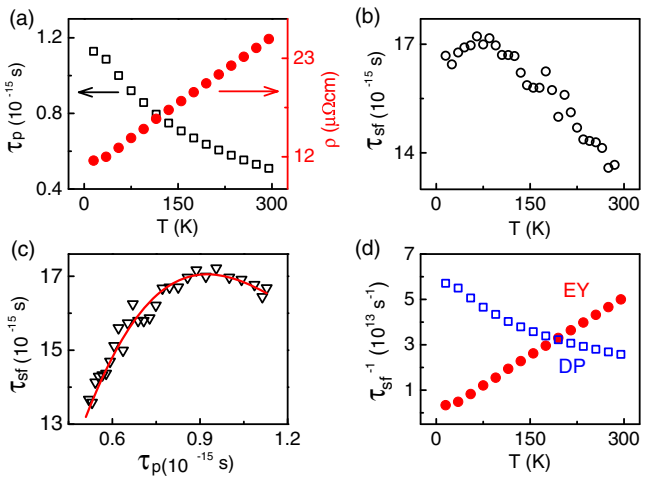

FIG. 2. (a) Bulk resistivity (right scale) and the momentum relaxation time (left scale) vs temperature for the studied Pt films. (b) Spin relaxation time vs temperature determined from the data of Fig. 1(c). (c) Spin relaxation time vs momentum relaxation time. Symbols: data, curve: fitting with a superposition of EY and DP-like contributions, as described in the text. (d) Temperature dependence of the contributions to spin relaxation from DP-like and EY mechanisms, as labeled, determined from the fitting in panel (c).

To interpret our results, we note that the strong intrinsic SHE in Pt [10,57] is attributed to the large spin Berry curvature of electron bands in the vicinity of nearly degenerate points, known as spin hot spots [57–59]. Large spin Berry curvature leads to strong spin mixing of electronic states at the hot spots, resulting in their complete spin depolarization [58]. Therefore, spin-polarized electrons injected into this states experience spin dynamics even in the absence of scattering. Since these dynamics depends on the wave vector, it must result in spin dephasing similar to the DP relaxation.

To quantify different contributions to spin relaxation in Pt, we use Matthiessen's rule $1/\tau_p = 1/\tau_{imp} + 1/\tau_{ph}(T)$ to separate the momentum relaxation rates $1/\tau_{imp}$ and $1/\tau_{ph}$ due to scattering on impurities and phonons, respectively. We fit the relationship between τ_{sf} and τ_p with $1/\tau_{sf} = 1/\tau_{DP} + 1/\tau_{EY}$, where $1/\tau_{DP} = (\Omega_{SO}^2 \tau_p)$ and $1/\tau_{EY} = b_{imp}^2/\tau_{imp} + b_{ph}^2/\tau_{phonon}$ are the DP-like and the EY contributions to spin relaxation [48]. Here, b_{imp} and b_{ph} are the effective spin mixing parameters associated with impurity and phonon scattering, respectively. For simplicity, we characterize the DP-like relaxation by an average effective spin-orbit field H_{SO}, with $\Omega_{SO} = g\mu_B H_{SO}/\hbar$ representing the average precession frequency around H_{SO}. The fitting [curve in Fig. 2(c)] allows us to estimate $H_{SO} \approx 1280 \pm 80$ T, $b_{imp} \approx 0.062 \pm 0.057$, and $b_{phonon} \approx 0.208 \pm 0.008$, where the uncertainties reflect the accuracy of the fitting.

The average precession phase, $\Omega\tau_p \approx 0.2$, between momentum scattering events satisfies the random spin-walk approximation used in our analysis. The probability of spin flipping per momentum scattering event, $P_{sf} = b^2/(1-b^2)$ [51], gives one spin flip per 25 (160) phonon (impurity) scattering events, consistent with the diffusive limit used in our analysis. At RT, the EY contribution to spin relaxation is about 2 times larger than the DP-like contribution [Fig. 2(d)]. The EY contribution decreases linearly with decreasing T, while the DP-like contribution increases, becoming larger than that of EY at temperatures below 195 K. With increasing purity of Pt, the DP-like contribution is expected to increase, while the EY contribution should decrease.

Further evidence for DP-like relaxation in Pt was provided by measurements of the nanopillar with an active spin valve structure Py(10)Pt(1)Cu(4)Py(5), where Pt was interfaced with Py. In this case, the MR linearly increases with decreasing temperature [triangles in Fig. 3(a)]. In contrast, for the standard structure with $d = 1$, the MR starts to decrease at low T [circles in Fig. 3(a)]. The downcurving of MR is also apparent in the VF calculations [solid curve in Fig. 3(a)], but is less significant, likely due to the limitations of the diffusive transport model and/or the

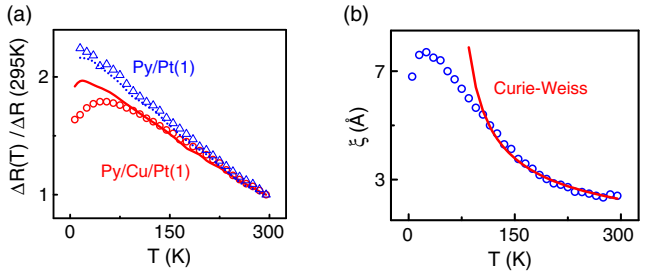

FIG. 3. (a) Measured (symbols) and calculated (curves) MR vs temperature for the standard spin valve nanopillar with $d = 1$ nm (circles and solid curve), and for the nanopillar with the structure Py(10)Pt(1)Cu(4)Py(5) (triangles and dotted curve). For the latter, the calculation includes only the EY contribution to spin relaxation. The MR is normalized by its value at RT. (b) Symbols: magnetic correlation length in Pt vs temperature, from Ref. [32]. Curve: dependence expected based on the Curie-Weiss law.

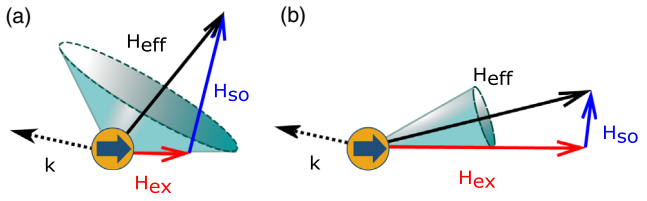

FIG. 4. Interplay between magnetism and intrinsic spin-orbit interaction. The spin of electron in Pt precesses around the effective field $\vec{H}_{\rm eff} = \vec{H}_{\rm SO} + \vec{H}_{\rm ex}$, where $\vec{H}_{\rm SO}$ is the effective spin-orbit field determined by the electron's momentum $\vec{k}$, and $\vec{H}_{\rm ex}$ is the effective exchange field due to either proximity-induced magnetism or magnetic fluctuation in Pt. The electron's spin is shown by a bold circled arrow. (a) If $H_{\rm SO}$ dominates, precessional dephasing suppresses the spin polarization and/or magnetization fluctuation. (b) If $H_{\rm ex}$ dominates, the precession angle for electron spins aligned with $\vec{H}_{\rm ex}$ is small, suppressing the DP-like spin relaxation.

discontinuity of the Pt(1) layer. Measurements and calculations for thicker Pt also showed downcurving of MR at low T, which can be attributed to the DP-like relaxation [39]. For Pt directly interfaced with Py, the linear dependence of MR on T without such downcurving indicates that DP-like relaxation is suppressed, which was confirmed by the VF calculation including only the EY mechanism [dotted curve in Fig. 3(a)].

The difference between the two structures can be correlated with the temperature-dependent magnetic properties of Pt, as illustrated in Fig. 3(b), reproduced from Ref. [32]. Symbols show the measured magnetic correlation length, and the curve shows the temperature dependence expected from the Curie-Weiss law, extrapolating to the Curie temperature of 90 K. The correlation length significantly deviates from the Curie-Weiss law at $T < 110$ K, and starts to decrease at $T < 25$ K, suggesting that magnetism in Pt becomes suppressed. Indeed, ferromagnetism was reported only in ultrathin Pt films and nanoparticles [60–62].

Both the effects of the magnetic interfaces on MR and the suppression of magnetism in Pt are observed at cryogenic temperatures, where the DP-like relaxation becomes increasingly significant [see Fig. 2(d)]. We explain these effects by the interplay between $H_{\rm SO}$ and the proximity-induced effective exchange field $H_{\rm ex}$. The electron's spin experiences precession around the total effective field, $\vec{H}_{\rm eff} = \vec{H}_{\rm SO} + \vec{H}_{\rm ex}$. If $H_{\rm ex} \ll \vec{H}_{\rm SO}$ away from magnetic interfaces, the spins of the diffusing electrons, characterized by a broad distribution of wave vectors, $\vec{k}$, are efficiently dephased by the dominant momentum-dependent DP-like field, Fig. 4(a). SOI-induced spin dephasing is likely responsible for the suppression of magnetism in Pt, since it competes with the exchange interaction that stabilizes an ordered-spin state of the Fermi sea comprising electrons with a broad distribution of $\vec{k}$.

If $H_{\rm ex} \gg H_{\rm SO}$, near a magnetic interface, the spin precesses around the effective field, $\vec{H}_{\rm eff}$, dominated by $\vec{H}_{\rm ex}$ [Fig. 4(b)]. Since the spins of the electrons injected from the ferromagnet are aligned with $\vec{H}_{\rm ex}$, their precession angle is small, resulting in suppression of the precessional spin relaxation, and thus an enhanced MR in the samples with proximity-magnetized Pt. This proposed mechanism is consistent with the reported suppression of DP relaxation by the external field [53], and with the reduction of intrinsic SHE in proximity-magnetized Pt [29].

Interplay between SOI and magnetism should also result in enhancement of proximity magnetism in Pt when SOI-induced spin dephasing is reduced. Indeed, magnetic coupling between ferromagnets, separated by a proximity-magnetized Pt spacer, was shown to monotonically increase with decreasing temperature [32], even though the magnetic correlation length decreases at low T [Fig. 3(b)]. This is consistent with nonlinear enhancement of magnetism in Pt in the immediate vicinity of the interface, where DP-like relaxation is suppressed, compensating for its more abrupt decrease away from the interface.

In conclusion, we utilized nanoscale magnetic spin valves to study spin transport and relaxation in Pt and at its interfaces with Cu. Analysis of spin relaxation allowed us to quantify the Elliott-Yafet scattering, and to identify a previously unrecognized Dyakonov-Perel-like intrinsic spin relaxation mechanism in Pt. Our analysis allowed us to estimate the average strength of the relevant spin-orbit parameters. We also demonstrated that spin-orbit effects compete with magnetism at the interfaces of Pt with ferromagnets, resulting in suppression of spin relaxation. Our results demonstrate an efficient route for the characterization of spin-orbit interactions, which should facilitate the exploration of new efficient spin-orbit materials.

This work was supported by the NSF Grants No. DMR-1350002 and No. DMR-1504449.

[1] D. Ralph and M. Stiles, J. Magn. Magn. Mater. **320**, 1190 (2008).
[2] S. A. Wolf, D. D. Awschalom, R. A. Buhrman, J. M. Daughton, S. von Molnar, M. L. Roukes, A. Y. Chtchelkanova, and D. M. Treger, Science **294**, 1488 (2001).
[3] S. Bader and S. Parkin, Annu. Rev. Condens. Matter Phys. **1**, 71 (2010).
[4] G. Bauer, E. Saitoh, and B. van Wees, Nat. Mater. **11**, 391 (2012).
[5] A. Manchon, H. Koo, J. Nitta, S. Frolov, and R. Duine, Nat. Mater. **14**, 871 (2015).
[6] M. D'Yakonov and V. Perel, J. Exp. Theor. Phys. Lett. **13**, 3023 (1971).
[7] L. Liu, O. J. Lee, T. J. Gudmundsen, D. C. Ralph, and R. A. Buhrman, Phys. Rev. Lett. **109**, 096602 (2012).
[8] C. Hahn, G. de Loubens, O. Klein, M. Viret, V. V. Naletov, and J. Ben Youssef, Phys. Rev. B **87**, 174417 (2013).
[9] J. Wunderlich, Nat. Mater. **16**, 284 (2017).
[10] L. Liu, R. A. Buhrman, and D. C. Ralph, arXiv:1111.3702.
[11] L. Liu, C.-F. Pai, Y. Li, H. W. Tseng, D. C. Ralph, and R. A. Buhrman, Science **336**, 555 (2012).
[12] C.-F. Pai, L. Liu, Y. Li, H. W. Tseng, D. C. Ralph, and R. A. Buhrman, Appl. Phys. Lett. **101**, 122404 (2012).
[13] Y. Niimi, Y. Kawanishi, D. H. Wei, C. Deranlot, H. X. Yang, M. Chshiev, T. Valet, A. Fert, and Y. Otani, Phys. Rev. Lett. **109**, 156602 (2012).
[14] J.-C. Rojas-Sanchez, N. Reyren, P. Laczkowski, W. Savero, J.-P. Attane, C. Deranlot, M. Jamet, J.-M. George, L. Vila, and H. Jaffres, Phys. Rev. Lett. **112**, 106602 (2014).
[15] K. D. Belashchenko, A. A. Kovalev, and M. van Schilfgaarde, Phys. Rev. Lett. **117**, 207204 (2016).
[16] L. Liu, T. Moriyama, D. C. Ralph, and R. A. Buhrman, Phys. Rev. Lett. **106**, 036601 (2011).
[17] C. Jaworski, R. Myers, E. Johnston-Halperin, and J. Heremans, Nature (London) **487**, 210 (2012).
[18] J. Bass and W. P. Pratt Jr., J. Phys. Condens. Matter **19**, 183201 (2007).
[19] F. D. Czeschka, L. Dreher, M. S. Brandt, M. Weiler, M. Althammer, I.-M. Imort, G. Reiss, A. Thomas, W. Schoch, W. Limmer, H. Huebl, R. Gross, and S. T. B. Goennenwein, Phys. Rev. Lett. **107**, 046601 (2011).
[20] W. Zhang, V. Vlaminck, J. E. Pearson, R. Divan, S. D. Bader, and A. Hoffmann, Appl. Phys. Lett. **103**, 242414 (2013).
[21] M. Isasa, E. Villamor, L. E. Hueso, M. Gradhand, and F. Casanova, Phys. Rev. B **91**, 024402 (2015).
[22] C. Stamm, C. Murer, M. Berritta, J. Fang, M. Gabureac, P. M. Oppeneeer, and P. Gambardella, Phys. Rev. Lett. **119**, 087203 (2017).
[23] W. Zhang, W. Han, X. Jiang, S.-H. Yang, and S. S. P. Parkin, Nat. Phys. **11**, 496 (2015).
[24] K. Roy, Phys. Rev. B **96**, 174432 (2017).
[25] H. Nguyen, W. P. Pratt Jr., and J. Bass, J. Magn. Magn. Mater. **361**, 30 (2014).
[26] M.-H. Nguyen, D. Ralph, and R. Buhrman, Phys. Rev. Lett. **116**, 126601 (2016).
[27] F. Hellman *et al.*, Rev. Mod. Phys. **89**, 025006 (2017).
[28] J. Ryu, M. Kohda, and J. Nitta, Phys. Rev. Lett. **116**, 256802 (2016).
[29] W. Zhang, M. B. Jungfleisch, W. Jiang, Y. Liu, J. E. Pearson, S. G. E. te Velthuis, A. Hoffmann, F. Freimuth, and Y. Mokrousov, Phys. Rev. B **91**, 115316 (2015).
[30] M. N. Baibich, J. M. Broto, A. Fert, F. Nguyen Van Dau, F. Petroff, P. Etienne, G. Creuzet, A. Friederich, and J. Chazelas, Phys. Rev. Lett. **61**, 2472 (1988).
[31] S. Y. Huang, X. Fan, D. Qu, Y. P. Chen, W. G. Wang, J. Wu, T. Y. Chen, J. Q. Xiao, and C. L. Chien, Phys. Rev. Lett. **109**, 107204 (2012).
[32] W. L. Lim, N. Ebrahim-Zadeh, J. C. Owens, H. G. E. Hentschel, and S. Urazhdin, Appl. Phys. Lett. **102**, 162404 (2013).
[33] S. Urazhdin, H. Kurt, W. Pratt Jr., and J. Bass, Appl. Phys. Lett. **83**, 114 (2003).
[34] C.-F. Pai, Y. Ou, L. H. Vilela-Leao, D. C. Ralph, and R. A. Buhrman, Phys. Rev. B **92**, 064426 (2015).
[35] T. Valet and A. Fert, Phys. Rev. B **48**, 7099 (1993).
[36] A. Fert and S.-F. Lee, Phys. Rev. B **53**, 6554 (1996).
[37] P. C. van Son, H. van Kempen, and P. Wyder, Phys. Rev. Lett. **58**, 2271 (1987).
[38] J. Bass and W. P. Pratt Jr., J. Magn. Magn. Mater. **200**, 274 (1999).
[39] See Supplemental Material at http://link.aps.org/supplemental/10.1103/PhysRevLett.120.067204 for details on the magnetoresistance calculations, which include Refs. [40–46].
[40] L. Vila, W. Park, J. A. Cabellero, D. Bozek, R. Loloee, W. P. Pratt Jr., and J. Bass, J. Appl. Phys. **87**, 8610 (2000).
[41] S. D. Steenwyk, S. Y. Hsu, R. Loloee, J. Bass, and W. P. Pratt Jr., J. Magn. Magn. Mater. **170**, L1 (1997).
[42] E. Villamor, M. Isasa, L. E. Hueso, and F. Casanova, Phys. Rev. B **88**, 184411 (2013).
[43] N. Ashcroft and N. Mermin, *Solid State Physics* (Cengage Learning, Boston, MA, 2011).
[44] E. Sondheimer, Adv. Phys. **1**, 1 (1952).
[45] K.-W. Kim, L. O'Brien, P. A. Crowell, C. Leighton, and M. D. Stiles, Phys. Rev. B **95**, 104404 (2017).
[46] R. E. Parra and R. A. Lopez, J. Appl. Phys. **61**, 3989 (1987).
[47] H. Kurt, R. Loloee, K. Eid, W. P. Pratt Jr., and J. Bass, Appl. Phys. Lett. **81**, 4787 (2002).
[48] I. Zutic, J. Fabian, and S. D. Sarma, Rev. Mod. Phys. **76**, 323 (2004).
[49] M. Dyakonov and V. Perel, Soviet Phys. Solid State, USSR **13**, 3023 (1972).
[50] P. M. Haney, H.-W. Lee, K.-J. Lee, A. Manchon, and M. D. Stiles, Phys. Rev. B **87**, 174411 (2013).
[51] P. Boross, B. Dora, A. Kiss, and F. Simon, Sci. Rep. **3**, 3233 (2013).
[52] C. Fang, C. H. Wan, B. S. Yang, J. Y. Qin, B. S. Tao, H. Wu, X. Zhang, X. F. Han, A. Hoffmann, X. M. Liu, and Z. M. Jin, Phys. Rev. B **96**, 134421 (2017).
[53] R. I. Dzhioev, K. V. Kavokin, V. L. Korenev, M. V. Lazarev, N. K. Poletaev, B. P. Zakharchenya, E. A. Stinaff, D. Gammon, A. S. Bracker, and M. E. Ware, Phys. Rev. Lett. **93**, 216402 (2004).
[54] H. Idzuchi, Y. Fukuma, L. Wang, and Y. Otani, Appl. Phys. Lett. **101**, 022415 (2012).
[55] G. Mihajlović, J. E. Pearson, S. D. Bader, and A. Hoffmann, Phys. Rev. Lett. **104**, 237202 (2010).

[56] T. Kimura, T. Sato, and Y. Otani, Phys. Rev. Lett. **100**, 066602 (2008).
[57] G. Y. Guo, S. Murakami, T.-W. Chen, and N. Nagaosa, Phys. Rev. Lett. **100**, 096401 (2008).
[58] M. Gradhand, D. V. Fedorov, F. Pientka, P. Zahn, I. Mertig, and B. L. Gyrffy, J. Phys. Condens. Matter **24**, 213202 (2012).
[59] H. Kontani, T. Tanaka, D. S. Hirashima, K. Yamada, and J. Inoue, Phys. Rev. Lett. **102**, 016601 (2009).
[60] A. Delin and E. Tosatti, Surf. Sci. **566–568**, 262 (2004).
[61] X. Teng, W.-Q. Han, W. Ku, and M. Hucker, Angew. Chem. **120**, 2085 (2008).
[62] M. J. B. J. Beille and D Bloch, J. Phys. F **4**, 1275 (1974).